

Supplementary Material

1 Supplementary Data

1.1 Method of the Digisonde Drift Measurements manual data calculation:

Besides modern digital ionosondes provide also routine ionospheric drift measurements in addition to classical vertical ionospheric sounding. Nowadays, tens of digisondes worldwide measure ionospheric drifts routinely and store their data in GIRO. Kouba et al. (2008) pointed to potential problems in the drift data processing applied earlier and proposed a methodology for the selection of correct source points to calculate a reliable drift velocity vector. They studied the basic characteristics for PQ station and observed daily and annual dependence of the vertical component of the drift velocity (Kouba and Koucka Knizova, 2016).

The Digisonde Drift Measurements (DDM) have three phases of processing. The primary output of the measurement is the spectra of the received signal for each sounding frequency and each antenna at the given height range. As a second product (skymap), individual reflection points in the ionosphere can be obtained from this data. Each such point then has specific properties – position in space, the Doppler shift value, sounding frequency, signal amplitude, SNR and others. The final product of the DDM is a vector of the plasma drift velocity (the value of the vertical and two horizontal components). We fit a velocity vector that best corresponds to the measured skymap (mostly using the least squares method, see Reinisch et al, 1998 for more details). During the calculation, we assume that the velocity field above the station can be described by a single velocity vector. The second assumption is that the detected reflection points on the skymap cover a sufficient part of the space above the station so that we are able to calculate all three components of the velocity vector. If, for example, only reflection points are detected near the vertical direction, a sufficiently accurate calculation is possible for the vertical component of the drift velocity only as the value of estimated horizontal components will be burdened by a big and mostly unacceptable error (see Kouba and Koucka Knizova, 2012).

Both mentioned assumptions are related to the character of the skymap. The assumption of a single velocity vector corresponds to a skymap with a "bipolar" pattern - the value of the Doppler shift changes smoothly from negative values on one edge of the skymap to positive values on the opposite edge. These skymaps correspond to a situation with a significant horizontal drift velocity component above the station. An example of such a skymap is in Supplementary Figure 4a. For such skymaps, all three components of the vector are calculated with sufficient accuracy. On the graphs of the drift velocity course, the points corresponding to these measurements are highlighted.

However, we don't always detect such skymaps. In cases where we measure other patterns of the skymap, it is necessary to consider whether it is possible to interpret the situation above the station as a single drift velocity vector. An example of such a skymap is in Supplementary Figure 4c. In the case of such a skymap, it would be misleading to interpret the drift using a single vector. A more complex model can be used to interpret the situation above the station - several independent drift velocity vectors, height dependence of the vector and others. Practically, such interpretations are not routinely performed. In the case of complex skymaps, we recommend not determining the horizontal components of the velocity vector and interpreting no more than the vertical component of the drift velocity (see Kouba and Koucka Knizova, 2016).

1.2 The daytime and nighttime happened exceptions between foF2 and TEC for storm 2012 and 2015

The daytime happened exceptions between foF2 and TEC for storm 2012 are detailed here: 1) on 14 Nov (main phase of storm) the TEC data shows not just negative phase at all station like foF2, but at AT it turns into positive; 2) on 15 Nov all station shows significant positive phase in TEC, but in foF2 JR just really slightly, closer to no deviation from the reference value (see Figure 2 and 4 and Supplementary Table 3).

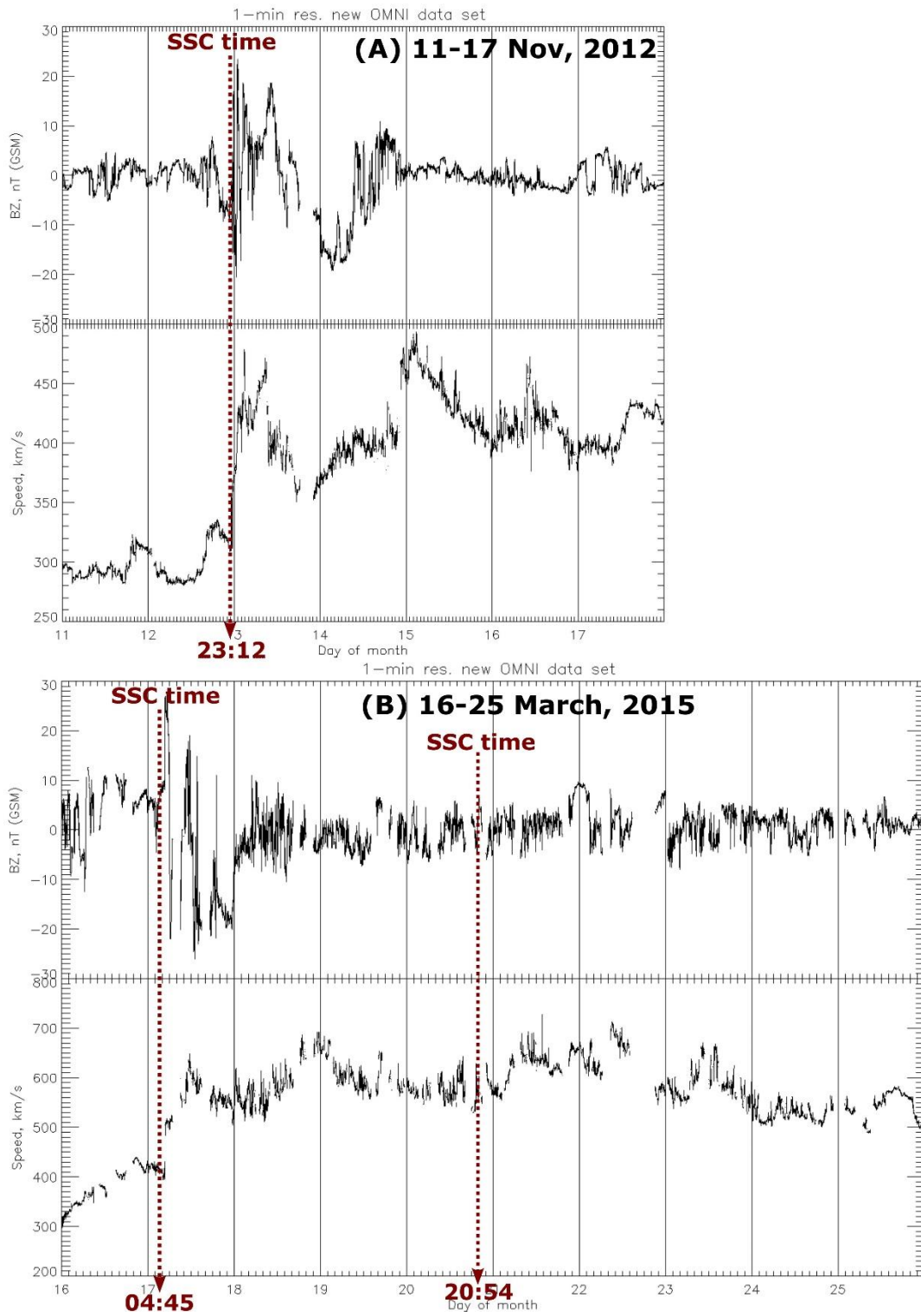
On the other hand, during the nighttime hours there were more differences between the behavior of the two ionospheric parameters: 1) on 12 November foF2 and TEC is decreased at all stations except at JR in TEC; 2) on 13 Nov TEC and foF2 showed an increase in electron density at all stations but the foF2 parameter turns to negative phase at SO, PQ and JR stations around midnight; 3) on 16 Nov TEC was not disturbed but the foF2 parameter was in a negative phase at PQ and JR, null at SO, and positive at AT, RO stations.

In the case of the 2015 storm, more pronounced difference was observed between the behavior of the foF2 and TEC data during the daytime (see also Figure 3 and 5): 1) on 17 March (main phase of storm) all stations had positive phase in TEC and in foF2 except for JR station. In foF2 a very short duration positive phase developed around noon (12 UT) that turned rapidly into negative at JR station. The turning time was delayed in TEC and occurred around 17 UT ; 2) on 18 March TEC dat all stations was negative, while foF2 only at JR, PQ, SO stations but positive at RO, AT; 3) on 22 and 23 March the TEC data showed a positive ionospheric storm phase at all stations, but foF2 remained quiet at JR and PQ and slightly positive at AT, RO, SO; 4) on 24 March all stations showed a positive phase in TEC, but no change in foF2 data.

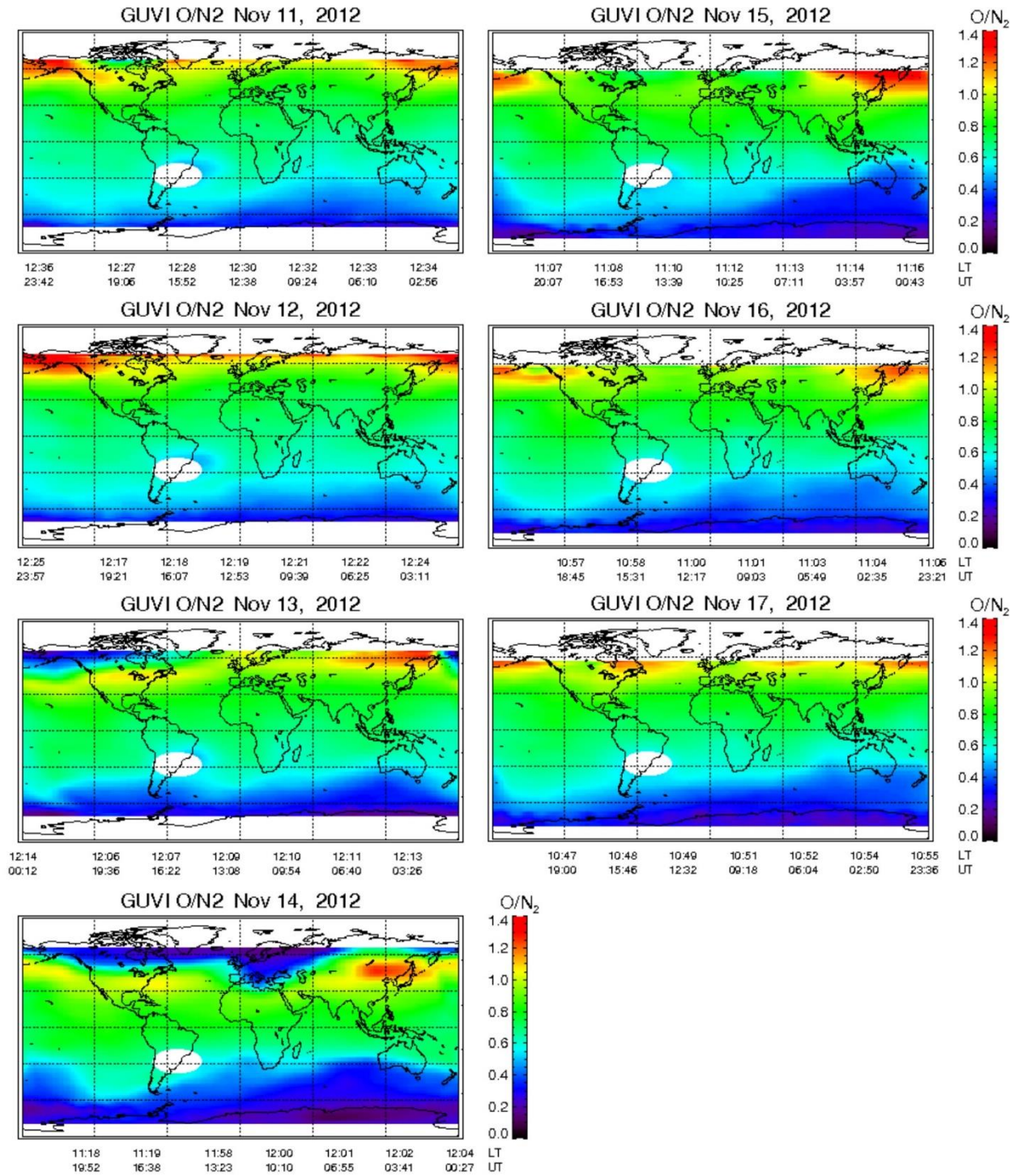
During the nighttime the following differences between foF2 and TEC trends were observed: 1) on 16 March no change was visible in TEC, but a positive phase emerged in foF2 at AT ,RO, JR; 2) on 22 March no change in TEC was observed, however, foF2 dropped into a negative phase at all stations except at RO. In the Supplementary Table 3 it can be seen that JR station behaves mostly differently.

2 Supplementary Figures and Tables

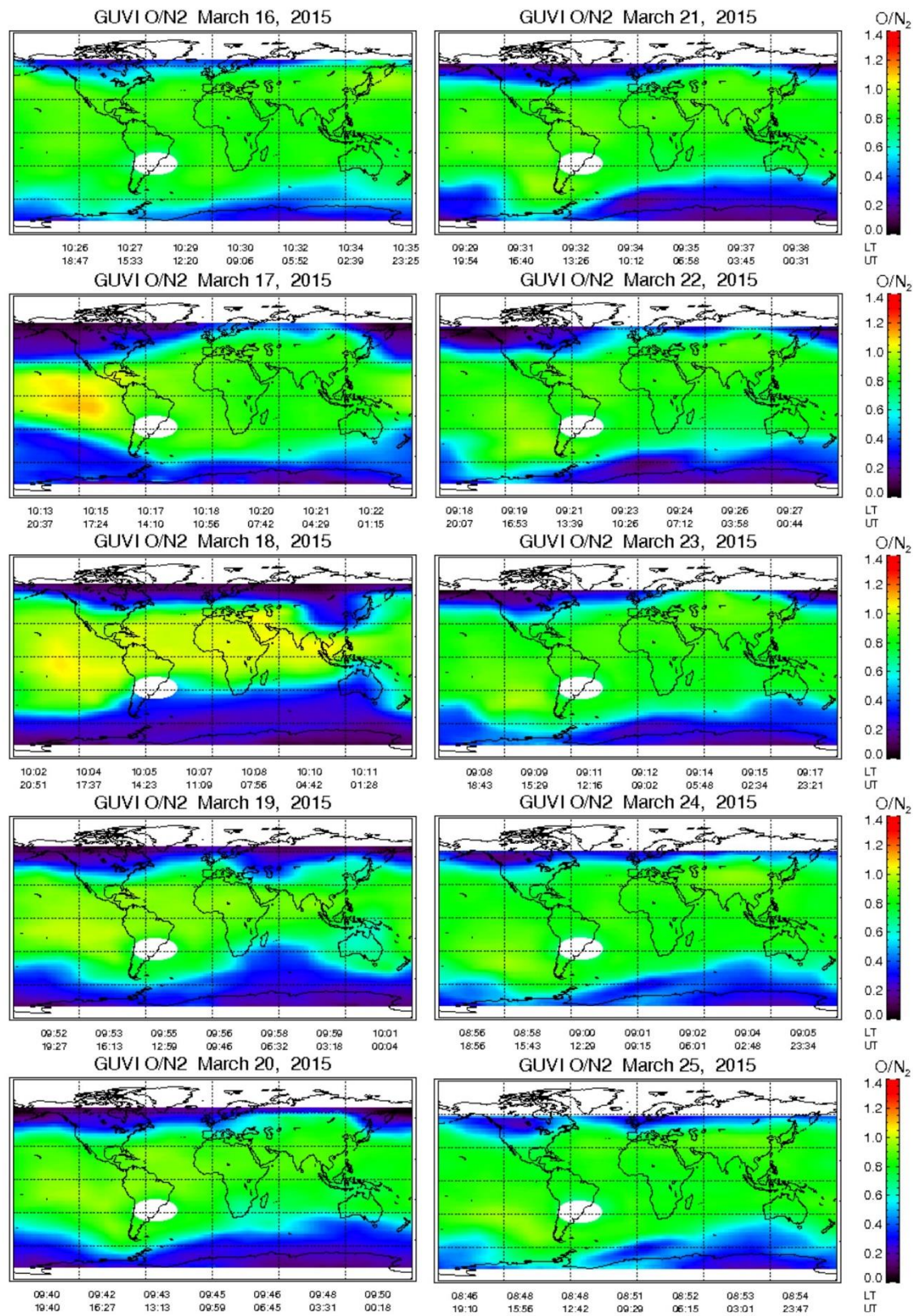
2.1 Supplementary Figures



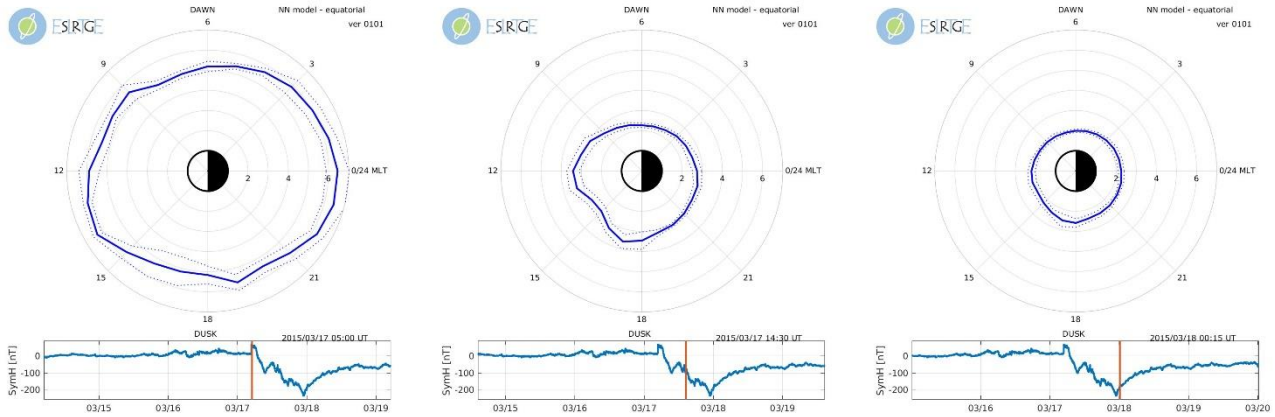
Supplementary Figure 1. 1-min resolution of the IMF Bz and solar wind speed data for the investigated storms. (A) is for the 2012 Nov, (B) is for the 2015 March storm.



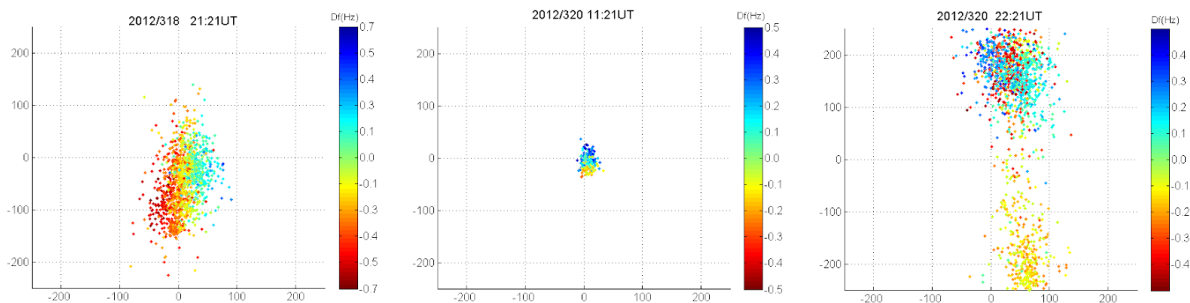
Supplementary Figure 2. The plot of GUVI data for the whole 2012 November storm



Supplementary Figure 3. The plot of GUVI data for the whole 2015 March storm



Supplementary Figure 4. Same UTs as in Figure 5, the equatorial cut of the plasmapause (our new empirical model)



Supplementary Figure 5. Examples of three types of skymaps: left panel - typical skymap with a "bipolar" pattern; for this pattern it is ideal to use the calculation of a single drift velocity vector. central panel - the detected reflection points are close to the vertical direction only. The analysis of the vertical drift velocity component is appropriate. The estimated horizontal components contain a large error. right panel - skymap with a "non-bipolar" pattern; it is not appropriate to use the assumption of a single drift velocity vector in this case.

2.2 Supplementary Tables

Sharp decrease in foF2 during the night, storm 2012					
Time [UT]	Athens (AT)	Rome (RO)	Sopron (SO)	Pruhonice (PQ)	Juliusruh (JR)
18:00			2.99		
18:15				2.95	
19:00	3.48				
19:43					2.10
19:45		3.45			
20:00-0:30			NaN		
20:28					1.75
20:43-22:13					NaN
20:45				1.68	
21:00-23:45				NaN	
1:00			1.90		
1:30	5.35				
2:30		5.55			

Supplementary Table 1. The appearance of the fade-out along the meridian on 14 November, 2012. The main stages of the temporal development of the fade-out events including the start of the decrease/increase (corresponding foF2 values are enhanced in green), the fade-out intervals (grey), the observed minima/maxima (corresponding foF2 in blue/red)

Sharp decrease in foF2 during the night, storm 2015					
Time [UT]	Athens (AT)	Rome (RO)	Sopron (SO)	Pruhonice (PQ)	Juliusruh (JR)
20:43					4.55
20:45				4.35	
21:43					2.45
22:00			3.87		
22:15				2.03	
23:00	4.60				
23:15		4.85	1.98		
0:00-01:00			NaN		
2:00		2.40			
2:15		NaN			
3:00-3:30			NaN		
3:15				1.80	
3:20	3.10				
4:13					2.35

Supplementary Table 2. The appearance of the fade-out along the meridian on 17 March, 2015. The main stages of the temporal development of the fade-out events including the start of the decrease/increase (corresponding foF2 values are enhanced in green), the fade-out intervals (grey), the observed minima (corresponding foF2 in blue)

(A) Type of the ionospheric storm phases								
2012	foF2 parameter				GNSS TEC			
Day of November	Daytime	Station	Nighttime	Station	Daytime	Station	Nighttime	Station
11	+	all	0	all	+	all	0	all
12	+	all	-	all	+	all	-	at AT, RO, SO, PQ
13	+	all	+	around midnight at SO, PQ, JR turn neg.	+	all	+	all
14	-	all	- ; +	neg. at SO, PQ, JR; pos. at AT, RO	- ; +	neg. at all except AT	- ; +	neg. At RO, SO, PQ, JR; pos. at AT
15	+	all except JR	-	all	+	all	-	all
16	+	all	- ; +	neg. at PQ, JR; pos. at AT, RO	+	all	0	all
17	+	all			+	all		
(B) Type of the ionospheric storm phases								
2015	foF2 parameter				GNSS TEC			
Day of March	Daytime	Station	Nighttime	Station	Daytime	Station	Nighttime	Station
16	0	all	+	AT, RO, JR	0	all	0	all
17	- ; +	neg at JR; pos. at AT, RO, SO, PQ	-	all	+	all	+0 ; -	just JR + and 0
18	- ; +	neg at SO, PQ, JR; pos. at AT, RO	-	all	-	all	-	all
19	-	all	-	all	-	all	-	all
20	-	all	-	all	-	all	-	all
21	-	all	-	all	-	all	0 ; -	just JR is 0
22	0 ; +	slight pos at AT, RO, SO	- ; 0	just AT, RO is 0	+	all	0	all
23	0 ; +	slight pos at AT, RO, SO, PQ	0 ; +	just JR is 0	+	all	0 ; +	just JR is 0
24	0	all	0 ; +	just JR is 0	+	all	+	all
25	0 ; +	slight pos at AT, RO, SO, PQ			+	all		

Supplementary Table 3. The ionospheric storm phases for the two examined storm intervals separated for daytime and nighttime groups. In the upper table (A) the foF2 and TEC data for the 2012 November storm is compared; in the lower plot (B) for the 2015 March storm